

DISTRIBUTION OF ICY PARTICLES ACROSS ENCELADUS' SURFACE AS DERIVED FROM CASSINI-VIMS MEASUREMENTS. K. Stephan¹, R. Jaumann¹, G. B. Hansen², R. N. Clark³, B. J. Buratti⁴, R. H. Brown⁵, K. H. Baines⁴, G. Bellucci⁶, A. Coradini⁶, D. P. Cruikshank⁷, C.A. Griffiths⁵, C. A. Hibbitts², T. B. McCord², R.M., Nelson⁴, P. D. Nicholson⁸, C. Sotin³, and R. Wagner¹. ¹ DLR, Inst. of Planet. Expl. Rutherfordstrasse 2, 12489 Berlin, Germany; ² Planetary Science Institute, 22 Fiddler's Rd., Winthrop WA 98862-0667; ³ USGS, Mail Stop 964, Box 25046, Denver Federal Center, Denver CO; ⁴ Jet propulsion Laboratory, Pasadena CA 91109; ⁵ Dept. Pl. Sci and LPL, U. of AZ, Tucson AZ 85721-0092; ⁶ Istituto Fisica Spazio Interplanetario, CNR, Via Fosso del Cavaliere, Roma, Italy; ⁷ NASA Ames Research Center, Astrophysics Branch, Moffett Field, CA 94035-1000; ⁸ Cornell University, 418 Space Sci. Bldg, Ithaca, NY 14853; ⁹ U. of Nantes, B.P. 92208, 2 rue de la Houssinière, 44072 Nantes Cedex 3, France (katrin.stephan@dlr.de).

Introduction: Compositionally, the surface of Enceladus is built up almost completely by water ice [1]. However, distinct variations in the size of water ice particles are apparent. As the band depths of water ice absorptions are sensitive to particle size, assuming constant abundance and viewing geometry, absorption depths can be used to map these variations across the surface. The Visual and Infrared Mapping Spectrometer [2] observed Enceladus with high spatial resolution during two Cassini fly-bys in 2005 (orbit 4 and 11). Based on these data we measured the band depths of water ice absorptions at 1.04, 1.25, 1.5 and 2 μm . The same procedure was applied to a water ice model developed by Hansen and McCord [3], which represents theoretically calculated reflectance spectra for a range of particle sizes between 1 μm and 1mm.

Spectral characteristics of water ice with different particle diameters: The spectral characteristic of water ice in the near-infrared wavelength region is well defined by distinct absorptions that increase in intensity with increasing wavelength (Fig 1). These absorptions vary in depth, mainly according to the wavelength variation of the refractive index of ice, to the particle diameter distribution of ice and to the amount of impurities in the surface material whose refractive indices are substantially different from those of water ice [4, 5]. The probability for a photon to be absorbed by an ice particle is higher if the ice particle is large, e.g. the distance through which light will travel in the ice particle is long. This effect causes the deepening of water ice absorptions and an increase in the reflectance slope between 1 μm and 3 μm with increasing particle diameter. Usually the surface ice of satellites is contaminated by impurities and absorption band depth variations depend also on this effect. However, the surface of Enceladus is mostly covered by pure crystalline water ice [1, 6] and variations of the band depths are mainly due to variations of the particle diameter. Therefore, in the particular case of Enceladus the band depths of the water ice absorptions can be used to map particle diameter variations across the surface. Figure 1 shows the spectral signature of a theoretical water ice spectrum with different particle diameter as derived from the model of Hansen and McCord.

The correlations of absorption depth and particle diameter show that specific band depths can be related to a specific particle diameter [7] (Fig. 2).

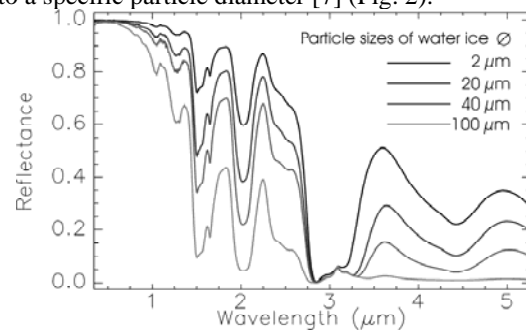


Fig. 1: Spectral signature of water ice with different particle diameters [3].

Furthermore, the short wavelength absorptions at 1.04 and 1.25 μm tend to be more sensitive to relatively large particles and the longer wavelength absorptions at 1.5 and 2 μm are more sensitive to the relatively small particles.

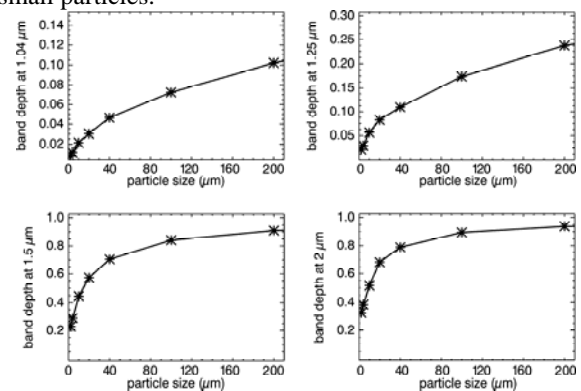


Fig. 2: Correlation between absorption band depths and particle diameter at 1.04 μm , 1.25 μm , 1.5 μm , and 2.0 μm of modeled water ice spectra [7].

Water ice particles on Enceladus: The spatial resolution of VIMS image cubes is sufficient to distinguish three major geologic units on Enceladus: heavily cratered terrain, ridged and fractured plains and complex tectonically deformed regions of troughs and ridges known as Sulci including the tiger stripes in the South Pole region. Although these geological units are assumed to be composed completely of water ice the band depths of the water ice absorptions changes significantly between these geological units. Each of

the geologic units exhibits its own characteristic range of water ice absorption band depths (Fig. 3).

Discussion: The largest particles are concentrated in the youngest and hottest surface regions on Enceladus. The distribution of icy particles unambiguously fits with morphological and geological terrain types. Although there are continuous transitions between the terrains, the heavily cratered terrain, fractured and ridged plains and the tectonically deformed regions each fall into a distinct particle diameter class. This suggests a correlation between the surface-forming processes and the development of the microstructure of the ice. Smallest particles are concentrated only in the heavily cratered terrain, which represent the oldest parts of Enceladus' surface. The largest particles are concentrated in the inner zones of the tectonically

deformed regions, which are the youngest geologic features on Enceladus. Surface ages, as derived from the impact flux models [8, 9, 10], can be correlated with the particle diameters (Fig. 4). From the distribution of particle diameters across the surface of Enceladus we can conclude that the largest particle diameters are inside the young tectonically deformed regions with a decrease in size outwards of the fractures. This is valid not only for the recent tiger stripes but also for older tectonically deformed regions. The relationship of a northward trending fracture zone with that of the tiger stripes and the associated particles size distribution in both areas suggests a probably genetic correlation.

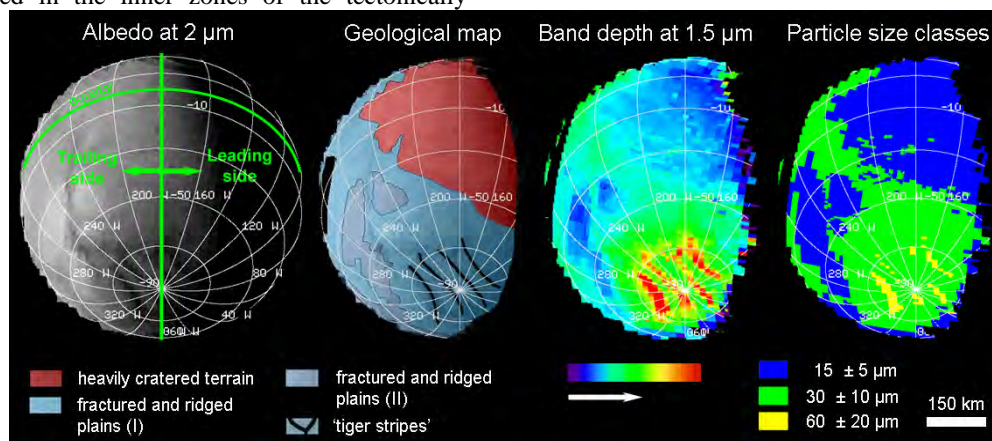


Fig. 3: VIMS cube image at 2 μm of the southern hemisphere (with a geologic map, absorption band depth at 1.5 μm and particle diameter classification. Hence this global mosaic shown here has a lower ground pixel resolution, the very small band of largest particles ($150 \pm 50 \mu\text{m}$) as indicated in red (map of absorption band depth at 1.5 μm) in the center of the tiger stripes cannot be resolved in the classification map. (Colors indicate from blue to red increasing absorption band depth (increasing particle diameter))

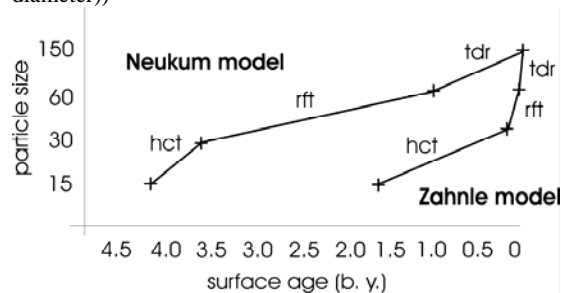


Fig. 4: Correlation of particle diameters and surface ages of the three terrain types: heavily cratered terrain (hct), ridged and fractured terrain (rft) and tectonically deformed regions (tdr). The ages are from Neukum (1985), Neukum et al. (2005) and Zahnle et al., (2003) impact flux models, respectively.

If the larger particles in the tectonically deformed regions are of cryovolcanic origin, the volcanic activity may have changed with time. With the South Polar Region as the youngest and partly still active zone and the older northward trending tectonic region

with its relatively large particles, we may see southward trending changes in the eruption history. However, there are still different possibilities to explain the observation: (1) The eruption zones and thus the internal heat distribution may have moved from north to south. (2) Cryovolcanic eruptions could have occurred all over the satellite and shrunk down with time to a small zone at the South Pole indicating a probable decrease in internal heat transfer. (3) The intensity of cryovolcanic eruptions was different at different locations and times with a maximum in the South Polar Region.

References: [1] Brown, R. B. et al. (2006) *Science*, 311. [2] Brown, R. B. et al. (2005) *Space Science Rev.* 115, 111. [3] Hansen, G. B. & McCord, T. B. (2004) *JGR*, 109. [4] Clark, R. and Lucey, P., (1984), *JGR* 89. [5] Dozier, J., (1989) G.Asars (ed.), *Wiley & Sons*. [6] Newman, S.F., et al., (2007), *Icarus*, submitted. [7] Jaumann, R., et al., (2007), *Icarus*, submitted. [8] Neukum, G., (1985) *Adv. Space Res.* 5. [9] Zahnle, K., et al., (2003), *Icarus*, 163. [9] Neukum, G., et al., (2005), *LPSC* 36, 2034.